

**ACUTE METEORITE DUST EXPOSURE AND PULMONARY INFLAMMATION - IMPLICATIONS FOR HUMAN SPACE EXPLORATION.** A.D. Harrington<sup>1,2,3</sup>, F.M. McCubbin<sup>1</sup>, J. Kaur<sup>3</sup>, A. Smirnov<sup>3,4</sup>, K. Galdanes<sup>2</sup>, M.A.A. Schoonen<sup>3,5</sup>, L.C. Chen<sup>2</sup>, S.E. Tsirka<sup>6</sup>, and T. Gordon<sup>2</sup>. <sup>1</sup>NASA Johnson Space Center, Mail Code XI2, Houston, TX 77058 (Andrea.D.Harrington@NASA.gov). <sup>2</sup>Department of Environmental Medicine, New York University School of Medicine, Tuxedo, NY 10987. <sup>3</sup>Department of Geosciences, Stony Brook University, Stony Brook, NY 11794. <sup>4</sup>Geology Department, Lone Star College, Kingwood, TX 77339. <sup>5</sup>Environmental Sciences Department, Brookhaven National Laboratory, Upton, NY 11973. <sup>6</sup>Pharmacological Sciences, Stony Brook University, Stony Brook, NY 11794.

**Introduction:** The previous manned missions to the Moon represent milestones of human ingenuity, perseverance, and intellectual curiosity. However, one of the major ongoing concerns is the array of hazards associated with lunar surface dust. Not only did the dust cause mechanical and structural integrity issues with the suits, the dust ‘storm’ generated upon reentrance into the crew cabin caused “lunar hay fever” and “almost blindness [1-3]” (Figure 1). It was further reported that the allergic response to the dust worsened with each exposure [4]. The lack of gravity exacerbated the exposure, requiring the astronauts to wear their helmet within the module in order to avoid breathing the irritating particles [1]. Due to the prevalence of these high exposures, the Human Research Roadmap developed by NASA identifies the *Risk of Adverse Health and Performance Effects of Celestial Dust Exposure* as an area of concern [5]. Extended human exploration will further increase the probability of inadvertent and repeated exposures to celestial dusts. Going forward, hazard assessments of celestial dusts will be determined through sample return efforts prior to astronaut deployment.



Figure 1. Eugene Cernan after a spacewalk (Apollo 17)

Studies on the lunar highland regolith indicate that the dust is not only respirable but also reactive [2, 6-9], and previous studies concluded that it is moderately toxic; generating a greater response than titanium oxide but a lower response than quartz [6]. The presence of reactive oxygen species (ROS) on the surface of the dust has been implicated. However, there is actually little data related to physicochemical

characteristics of particulates and pulmonary toxicity, especially as it relates to celestial dust exposure.

As a direct response to this deficit, the present study evaluates the role of a particulate’s innate geochemical features (e.g., bulk chemistry, internal composition, morphology, size, and reactivity) in generating adverse toxicological responses *in vitro* and *in vivo*. This highly interdisciplinary study evaluates the relative toxicity of six meteorite samples representing either basalt or regolith breccia on the surfaces of the Moon, Mars, and Asteroid 4Vesta (Table 1); three potential candidates for future human exploration or colonization. Terrestrial mid-ocean ridge basalt (MORB) is also used for comparison as a control sample.

**Table 1. Key Sample Information**

	Sample	Class	Description
Martian	Tissint	IB	Representative of starting conditions of rocks on Mars
	NWA 7034	RB	First sample of lithified Martian soil for study on Earth
Lunar	NWA 4734	IB	Representative of Mare regions and the starting conditions of lunar rocks
	NWA 7611	RB	Mechanical mixture of all the different rock types on the lunar surface
Vestian	Berthoud	IB	Primarily represents minimally processed, basaltic igneous material
	NWA 2060	RB	Representative of multiple generations of secondary processing
MORB		IB	Minimal secondary processing
IB (Igneous Basalt); RB (Regolith Breccia); H (Howardite); MORB (Terrestrial Mid-Ocean Ridge Basalt)			

**Experimental Details:** The meteorite and terrestrial samples were first crushed using an agate mortar and pestle and then ground using an agate ball mill to a respirable size fraction (<10 $\mu$ m). The bulk chemistry and mineralogy were determined via x-ray fluorescence and x-ray diffraction, respectively. The geochemical reactivity of the dust was evaluated by quantifying iron solubility (FerroZine UV-Vis method) and *in situ* reactive oxygen species (ROS) generation (ISO-HPO-100 Microsensor for hydrogen peroxide). Both *in vitro* and *in vivo* toxicological techniques were used to determine the pulmonary inflammation caused by acute exposure (hereafter

referred to as acute pulmonary inflammation or API). The *in vitro* method utilized a technique first published in [10], where the inflammatory stress response (ISR) of the cells to the presence of the dust is quantified. *In vivo* dust exposure was administered via oropharyngeal aspiration of dust slurries. The neutrophil infiltration into the bronchoalveolar lung fluid (BALF) was quantified to evaluate the body's inflammatory pulmonary response to the presence of the particles.

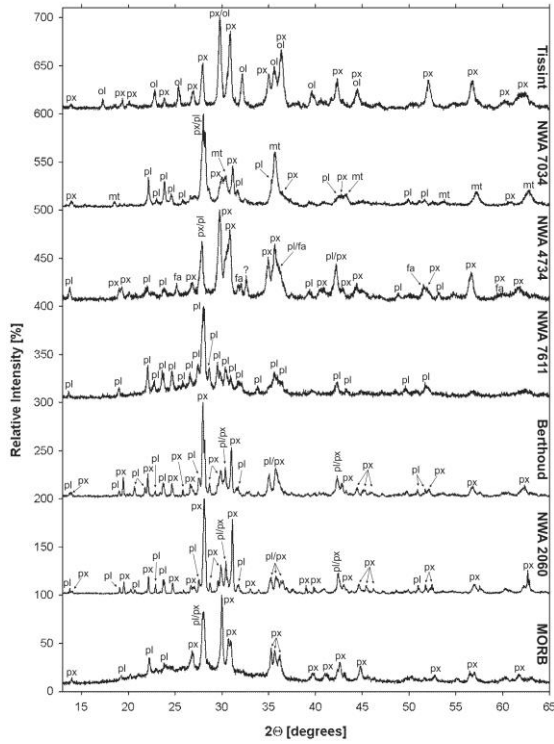


Figure 2. Mineralogical characterization of meteorite and MORB sample determined by XRD.

**Geochemical Results:** MORB, Tissint, and NWA 4734, all basalts, leached the most iron after eight days (Figure 2). NWA 7611, a lunar breccia, leached the least after eight days but based on the temporal trend, there was likely some iron precipitation from solution. Tissint and MORB also generated the greatest  $H_2O_2$  in solution. Within the first five minutes both generated 5  $\mu M$   $H_2O_2$ , after which the two differentiated with  $H_2O_2$  concentration 10  $\mu M$  after 20 minutes in the Tissint slurry. At 4  $\mu M$ , the NWA 4734 slurry generated the third highest concentration of  $H_2O_2$  in solution after 20 minutes.

**Biological Response Results:** The MORB generated the lowest ISR after 24 hours; followed by the lunar breccia NWA 7611 (Figure 3). The ISR values generated by NWA 7611 and the vestian samples are similar to inert material; however the

temporal trends indicate biological reactivity. The lunar basalt, NWA 4734, was the first dust sample to

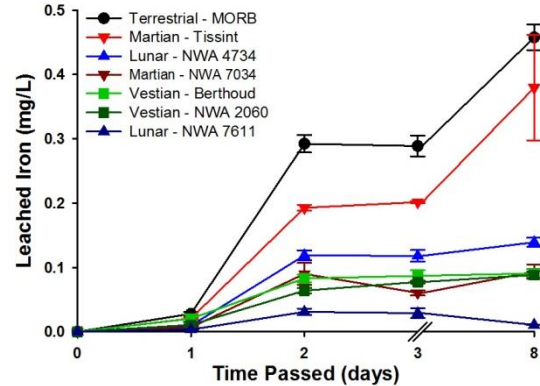


Figure 3. Iron leached from dust slurry (0.01  $m^2/mL$ ) in simulated lung fluid. For some data points, the error bars (SEM) are obscured by the symbols.

generate an ISR definitively outside of the range of inert material. The only other meteorite dust sample to generate a more significant loss in cell viability is the martian basalt, Tissint. Tissint also generated the second highest cellular upregulation of ROS, which was the major determining factor in its high ISR. The highest ISR and cellular upregulation of ROS was generated by the martian regolith, NWA 7034. Unlike Tissint, NWA 7034 did not illicit significant cellular death. However, although driven solely by the upregulation of ROS, the ISR generated by the NWA 7034 is similar to terrestrial soil contaminated with high levels of trace elements (NIST 2710 [10]).

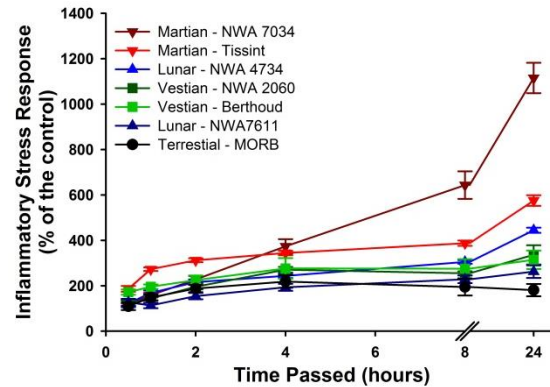


Figure 4. The ISR generated over time by the meteorite and terrestrial dust samples at a dose of 0.002  $m^2/mL$ . For some data points, the error bars (SEM) are obscured by the symbols.

The lunar basalt (NWA 4734) generated the greatest PMN infiltration into BALF followed by Tissint, the martian basalt. However, this difference was not statistically significant. The martian and lunar regolith dust samples generated the next greatest PMN infiltrations, respectively. These values are

statistically lower than Tissint but not from each other or from the NWA 2060 (Table S3). MORB generated the lowest PMN infiltration; statistically lower than all dust samples other than Berthoud.

**Discussion:** The MORB demonstrated higher geochemical reactivity than most of the meteorite samples but caused the lowest API (Table 2). Notably, the martian meteorites generated two of the three the highest API but only the basaltic sample is significantly reactive geochemically. Furthermore, while there is a correlation between a meteorite's soluble iron content and its ability to generate acellular ROS ( $P=0.0442$ ), there is no direct correlation between a particle's ability to generate ROS acellularly and its ability to generate API. However, assorted *in vivo* API markers (data not shown) did demonstrate strong positive correlations with Fenton metal content and the ratio of Fenton metals to silicon.

**Table 2. Sample Data Comparison to MORB**

Sample	Iron <sup>a</sup>	H <sub>2</sub> O <sub>2</sub> <sup>b</sup>	ISR <sup>c</sup> % of MORB	PMNs <sup>d</sup>
Tissint	83	208	618	163
	20	4	318	132
NWA 4734	30	83	246	172
NWA 7611	2	28	145	128
Berthoud	20	11	180	106
NWA 2060	19	53	174	120

<sup>a</sup> Iron leached from dust in simulated lung fluid after 8 days  
<sup>b</sup> H<sub>2</sub>O<sub>2</sub> formed in water after 25 minutes  
<sup>c</sup> Cellular ISR at 24 hours post exposure only  
<sup>d</sup> Polymorphonuclear leukocytes (PMNs) infiltration in BALF

In summary, this comprehensive dataset allows for not only the toxicological evaluation of celestial materials but also clarifies important correlations between geochemistry and health. Furthermore, the utilization of an array of celestial samples from Moon, Mars, and asteroid 4Vesta enabled the development of a geochemical based toxicological hazard model that can be used for: 1) mission planning, 2) rapid risk assessment in cases of unexpected exposures, and 3) evaluation of the efficacy of various *in situ* techniques in gauging surface dust toxicity.

**References:** [1] Armstrong A.E. and Collins M. (1969) NASA JSC, 81. [2] Cain, J.R. (2010) *Earth Moon and Planets*, **107**, 107-125. [3] Sheenan T. (1975) JSC-09432. [4] Scheuring T. et al. (2008) *Acta Astronautica* **63**, 980-987. [5] Scully R.R. et al. (2015) *HRP SHFH Element*. [6] Lam C.W. et al. (2013) *Inhal Tox* **25**, 661-678. [7] Lam C.W. et al. (2002) *Inhal Tox* **14**, 917-928. [8] Lam C.W. et al. (2002) *Inhal Tox* **14**, 901-916. [9] McKay D.S. et al. (2015) *Acta Astronautica* **107**, 163-176. [10] Harrington A.D. et al. (2010) *Geochem Trans* **13**.